J Radioanal Nucl Chem (2014) 302:701–707
DOI 10.1007/s10967-014-3271-2

Parameter optimization and experiment verification for a beta radioluminescence nuclear battery

Liang Hong · Xiao-Bin Tang · Zhi-Heng Xu · Yun-Peng Liu · Da Chen

Received: 15 April 2014 / Published online: 22 June 2014
© Akadémiai Kiadó, Budapest, Hungary 2014

Abstract In a beta radioluminescence nuclear battery, the beta energy is converted to light with the phosphor material, and then to electricity via photovoltaic cells. A method to optimize the thickness of phosphor layer is established in this study; the match between the luminescence spectrum and the photovoltaic cell is analyzed. The optimal parameters and output performance of the nuclear battery based on a sandwich-structure ^{147}Pm/ZnS:Cu/photovoltaic cell are determined with the MCNP, transport theory of light, and detailed balance limit of efficiency. The battery prototypes are fabricated and tested, and the experimental optimal thickness matches that of the theoretical result well.

Keywords Beta radioluminescence nuclear battery · Phosphor layer · Monte Carlo method · Transport theory of light · Detailed balance limit of efficiency

Introduction

The development of micro-electromechanical systems (MEMS) has increased the demand for power. However, traditional batteries, such as fuel and solar cells, cannot meet the demands of MEMS devices for power because of their large volume, short lifetime, and poor environmental adaptability [1]. The micro-radioisotope battery is a prime candidate for MEMS power supply due to its prolonged operation, high energy density, and good stability [2]. The beta radioluminescence nuclear battery or beta indirect-conversion nuclear battery, which is a radioisotope battery, can realize microminiaturization. This battery utilizes beta radioactive decay to produce luminescence in the phosphor material. Luminescence can then be collected and converted to electricity via a photovoltaic cell. The beta radioluminescence nuclear battery has several advantages, including high tolerance for ionizing radiation [3] and use of high-energy particles.

For efficient energy conversion, ZnS base phosphors with high radioluminescence efficiency and III–V semiconductors with low electrical leakage as photovoltaic cells should be employed [4]. Sims et al. [5] researched GaP power conversion with illumination by a ZnS:Ag light source and has demonstrated that GaP had a 23.54 and 14.59 % conversion efficiency under 968 and 2.85 μW cm^{-2} 440 nm blue light, respectively. Walko et al. [4] designed the radioluminescent photoelectric power sources base on the ^{3}H/ZnS aerogel composite light source and different photovoltaic cells. The power source volume and cost were estimated and the research showed that III–V design had the smaller volume, but the hydrogenated amorphous silicon design was less expensive. Sychov et al. [6] fabricated a ^{238}Pu/ZnS/AlGaAs indirect-conversion radioisotope battery with 0.11 % energy efficiency and 21 μW power output. Prelas et al. [7, 8] manufactured optoelectronic betavoltaic cells base on ^{85}Kr source and diamond photovoltaics. ^{85}Kr decays to produce electronic. The electronic excited the surrounding ^{85}Kr gas to generate Kr_2* and the photon with wavelength of 147 nm was emitted by Kr_2*. This work indicated that the using of wide bandgap photovoltaics in nuclear energy is a promising application. Schott [9] researched an energy conversion device by using photovoltaic cell and excimer gas-based photon source, and the study demonstrated power variations with gas pressure and

L. Hong · X.-B. Tang (✉) · Z.-H. Xu · Y.-P. Liu · D. Chen
Department of Nuclear Science and Engineering, Nanjing University of Aeronautics and Astronautics, Nanjing 210016, China
e-mail: tangxiaobin@nuaa.edu.cn

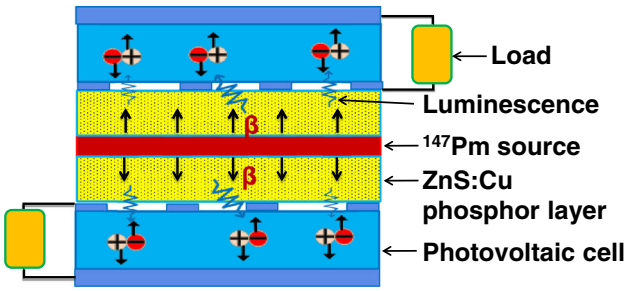

Fig. 1 Beta radioluminescence nuclear battery design model

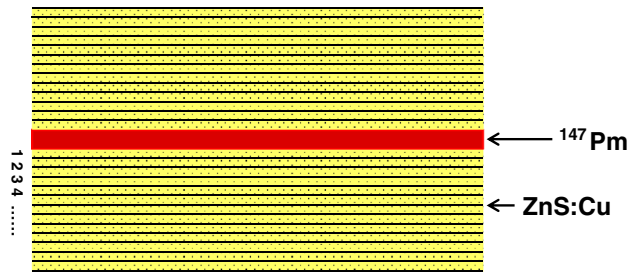

Fig. 2 Calculation model of radioluminescent light source

no radiation damage to the photovoltaic cell over a period in excess of 150 h. Weaver [10] presented the work on photon intermediate direct energy conversion systems using the α-emitter Po-210 (PIDECα) in his doctoral dissertation, and investigated the behavior of two proof-of-concept PIDEC devices using a rare gas fluorescer and a solid-state semiconductor crystal and demonstrated that the gas fluorescer system are encouraging. However, the conversion efficiency of this type nuclear battery is much lower than the predicted 25 % [11].

A beta radioluminescence nuclear battery based on a sandwich-structure ^{147}Pm/ZnS:Cu/photovoltaic cell is presented in this study. The optimization of the thickness of phosphor layer and the match between the luminescence spectrum and the bandgap (E_g) of photovoltaic cell may enhance the battery performance and conversion efficiency. The optimal thickness of the ZnS:Cu phosphor layer and optimal E_g of the photovoltaic cell are determined with MCNP, transport theory of light and detailed balance limit of efficiency. Battery prototypes were assembled and tested to verify the accuracy of the theoretical calculation. The experimental results fit the theoretical calculation value well.

Design model and theoretical calculation

A beta radioluminescence nuclear battery model with a sandwich-structure and bidirectional isotope ^{147}Pm sheet with a density of 7.4 g cm^{-3} (Fig. 1) was presented to fully utilize the source energy. The battery model is a square cell with a cross-sectional area of 1 cm^2. Figure 1 illustrates the power generation principle and nuclear battery process. The thickness of ^{147}Pm source was established through MCNP. The calculation model of the radioluminescent light source was established through MCNP (Fig. 2). In the MCNP calculation, the beta energy spectrum of ^{147}Pm was utilized and *F8 card was used to calculate energy deposition. By changing the thickness of the ^{147}Pm source (D_L), the conversion efficiency of decay energy into the energy of the beta flux emitted from the surface of the ^{147}Pm source (η_β) and the specific power of beta flux dP_β through elementary area dS (dP_β/dS) were obtained.

Only the upper portion of the battery model was analyzed in this study due to the symmetrical structure. The phosphor layer was subdivided into 90 μm boxes and was shown in Fig. 2. Every box is a 1 cm × 1 cm square and with a thickness of 0.367 mg cm^{-2} (2.25 μm). The boxes were labeled in a numerical order from inside (approaching ^{147}Pm) to outside (approaching the photovoltaic cell). The luminescence can be considered to generate in the center of each box. The process of conversion from energy deposited to photons created can express as follow: the phosphor layer absorb the kinetic energy of beta rays to generate high-energy electrons and holes, and cause low-energy excitation due to relaxation. Low energy electrons migrate in the phosphor layer and transmit the energy to the luminescence center (e.g. cupric ion). The recombination of electrons and holes occurs in the luminescence center and make it into the excited state, and accompany with light emission. The luminescence intensity produced from the nth box ($I(n)$) can be calculated by [12]

$$I(n) = E(n) \cdot \frac{h\nu}{2.67E_g + 0.87}, \quad (1)$$

where $E(n)$ is the energy deposition of the nth box, $h\nu$ is the energy of the photon emitted at the spectrum maximum, and E_g is the bandgap energy of the phosphor. For ZnS:Cu phosphor, $h\nu$ is equal to 2.3 eV and E_g is equal to 3.8 eV [12].

Luminescence is absorbed and scattered in the phosphor layer, and finally emitted from the phosphor layer surface and completely absorbed by the photovoltaic cell and the source. Luminescence is isotropic in the phosphor layer; thus, for the nth box, the luminescence intensity toward the photovoltaic cell ($I_{o,0}$) and the source ($I_{i,0}$) is expressed as follow:

$$I_{o,0}(n) = I_{i,0}(n) = 0.5I(n). \quad (2)$$

$I_{o,0}$ emitted from the external surface of the phosphor layer (toward the photovoltaic cell) with an intensity of I_1,

and simultaneously scattered toward the source with an intensity of $I_{i,1}$. These two can be calculated by [13]

$$I_1(n) = I_{o,0}(n)e^{-(a+s)(N-n+0.5)}, \quad (3)$$

$$I_{i,1}(n) = I_{o,0}(n)\left[e^{-a(N-n+0.5)} - e^{-(a+s)(N-n+0.5)}\right], \quad (4)$$

where a, s, and N are the absorption coefficient, scattering coefficient, and total number of the boxes, respectively. N ranges from 1 to 90, and n ranges from 1 to N. $I_1(n)$ is absorbed by the photovoltaic cell completely and will no longer enter the phosphor layer. By this time, the luminescence intensity toward the source is

$$I_{i,2}(n) = I_{i,0}(n)+I_{i,1}(n). \quad (5)$$

$I_{i,2}(n)$ is scattered toward the photovoltaic cell. The intensity can be calculated by

$$I_{o,1}(n) = I_{i,2}(n)\left[e^{-a(n-0.5)} - e^{-(a+s)(n-0.5)}\right]. \quad (6)$$

$I_{o,1}$ is then emitted from the external surface of the phosphor layer with an intensity of I_2, and scattered toward the source with an intensity of $I_{i,3}$, that is,

$$I_2(n) = I_{o,1}(n)e^{-(a+s)(N-n+0.5)}, \quad (7)$$

$$I_{i,3}(n) = I_{o,1}(n)[e^{-a(N-n+0.5)} - e^{-(a+s)(N-n+0.5)}]. \quad (8)$$

$I_2(n)$ is absorbed by the photovoltaic cell completely, and $I_{i,3}$ is scattered toward the photovoltaic cell. This cycle is then repeated. We only analyzed the luminescence emitted from the external surface of the phosphor layer. Therefore, the total luminescence intensity absorbed by the photovoltaic cell $(I_O(N))$ can be calculated as

$$I_O(N) = \sum_{n=1}^{N}\sum_{x=1}^{\infty} I_x(n). \quad (9)$$

a and s satisfy [13, 14]

$$a + s = \frac{\ln\frac{1}{T}}{l}, \quad (10)$$

$$\frac{a}{s} = \frac{(1-R_\infty)^2}{2R_\infty}, \quad (11)$$

where T, l and R_∞ are transmittance, thickness of the phosphor layer, and scattering rate, respectively. A photovoltaic cell was utilized for the conversion of luminescence into electricity. Theoretically, according to the Shockley diode equation, the output current density can be expressed as [15]

$$J(V) = J_{sc} - J_0\left[\exp(\frac{qV}{k_B T_a}) - 1\right], \quad (12)$$

where J_{sc} is the short-circuit current density, J_0 is the reverse saturation current density and V is the output voltage. J_{sc} and J_0 are expressed as follows:

$$J_{sc} = q\int_{E_g}^{\infty} b_s(E, T_a)dE, \quad (13)$$

$$J_0 = q\int_{E_g}^{\infty} \frac{2F_a E^2}{h^3c^2[\exp(\frac{E}{k_B T_a}) - 1]}dE, \quad (14)$$

where $b_s(E, T_a)$ is the photon flux density of luminescence that can be obtained through the luminescence spectrum of the ZnS:Cu phosphor layer (Fig. 3) and $I_O(N)$ (Eq. 9); q is the elementary charge, F_a is the environmental geometrical factor that is equal to π [15], T_a is the environment temperature that is equal to 300 K, h is Planck's constant, c is the speed of light in a vacuum, and k_B is the Boltzmann constant.

The open-circuit voltage (V_{oc}), output power density (P), and the total conversion efficiency of the beta radioluminescence nuclear battery (η_T) can be expressed as follows [16]:

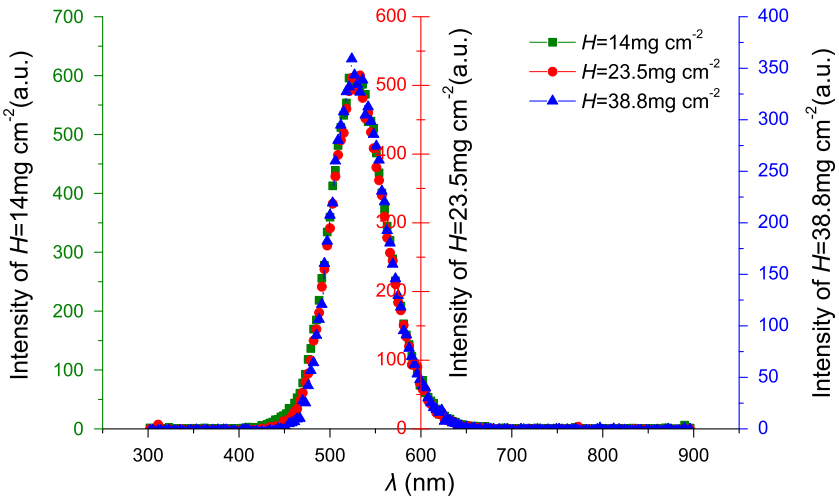

Fig. 3 Luminescence spectra of ZnS:Cu phosphor layers under ^{147}Pm excitation

$$V_{oc} = \frac{k_B T_a}{q} \cdot \ln\left(\frac{J_{sc}}{J_0} + 1\right), \quad (15)$$

$$P = J(V) \cdot V, \quad (16)$$

$$\eta_T = \frac{P_{max}}{AE_\beta}, \quad (17)$$

where P_{max} is the maximum output power density of the beta radioluminescence nuclear battery, A is the activity of the radioactive source, and E_β is the average beta energy of 62 keV for ^{147}Pm. J_{sc}, V_{oc}, P_{max} and η_T with the thickness of the phosphor layer (H) were calculated through MATLAB.

Results and discussion

Thickness of ^{147}Pm source in this study

Figure 4 shows the dependence of dP_β/dS, η_β and their products ($dP_\beta/dS \cdot \eta_\beta$) on D_L by MCNP. dP_β/dS increases and η_β decreases with the increase of D_L. D_L is denoted as 5.92 mg cm^{-2} in this study in accordance with the maximum value of $dP_\beta/dS \cdot \eta_\beta$. At this point, dP_β/dS reaches 70.3 % of the maximum value, and η_β is equal to 51 %. These high percentages can guarantee the high power output density and high conversion efficiency of the battery.

Optimal thickness of the ZnS:Cu phosphor layer (H_{op}) and optimal E_g

The phosphor layer transfers energy deposition as luminescence. The luminescence spectra of ZnS:Cu phosphor layers (prepared in an experiment) with ^{147}Pm excitation were measured with a Cary Eclipse luminescence spectrophotometer (Agilent Technologies, USA), as show in Fig. 3. According to the normalization luminescence spectra, luminescence intensity ($I_O(N)$) and Shockley diode equation (Eq. 12), the conversion efficiency of the nuclear battery may be calculated. Figure 5 shows η_T with H and E_g values. When H is increased, η_T initially increases rapidly and then declines gradually. This trend is explained by the different extents of absorption between the beta particle and luminescence in the phosphor layer. For the continuous beta spectrum of the ^{147}Pm source, the beta absorption curve is approximately the exponential curve [17]; thus, the increase in luminescence intensity will be reduced sharply by increasing H. While the increase in the absorption of luminescence will decrease slightly by increasing H. Consequently, the trend of η_T with different H initially increases rapidly and then declines gradually.

When H is equal to 11 mg cm^{-2} (H_{op}), η_T reaches the maximum value and H_{op} is independent of the value of E_g (Fig. 5). $I_O(N)$ reaches the maximum value at H_{op} as indicated by the MATLAB calculation. So J_{sc} and V_{oc} also reach the maximum value at H_{op} from Eqs. 13 and 15. When E_g is determined, J_0 is a constant. $J(V)$ increases with the increase in J_{sc} under the same V from Eq. 12. Therefore, P reaches the maximum value at H_{op} and is independent of E_g, and it is similar to η_T.

η_T initially increases and then decreases with the increase in E_g (Fig. 5). The entire luminescence spectrum of the ZnS:Cu phosphor layer ranges from 470 to 620 nm. The corresponding photon energy range is from 2.64 to 2 eV. The photovoltaic cell collects all photons within the entire luminescence spectrum with increasing E_g from 0 to

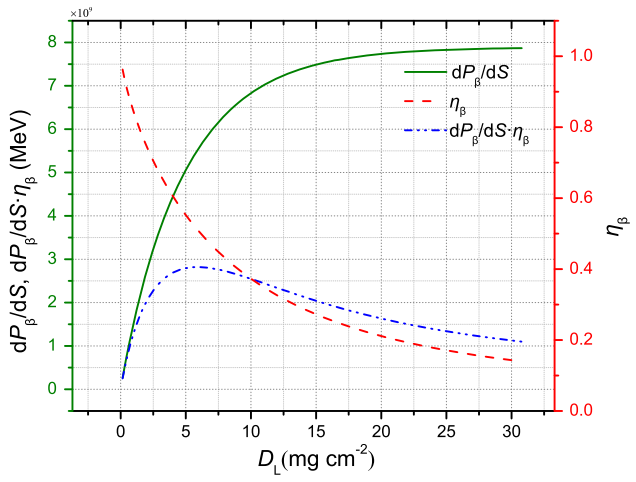

Fig. 4 The conversion efficiency of decay energy into the energy of the beta flux, the specific power of beta flux dP_β through elementary area dS, and their products

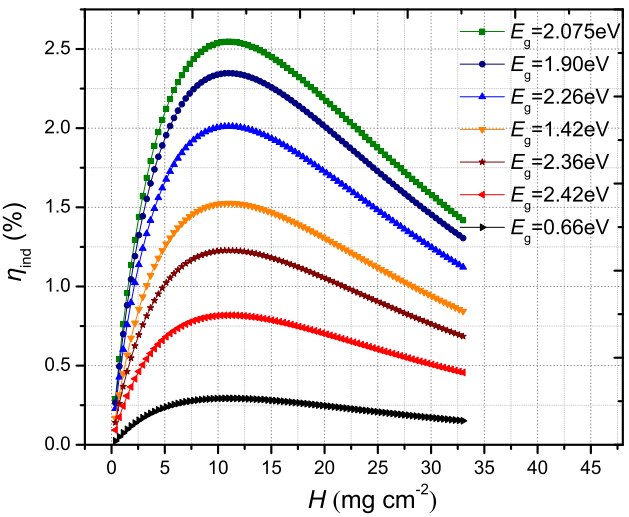

Fig. 5 Total conversion efficiency of the battery with different H and E_g value

2 eV. As shown in Eq. 13, J_{sc} remains the same with the increase in E_g. J_0 decreases with the increase in E_g, whereas V_{oc} from Eqs. 14 and 15 increases. $J(V)$ increases with the decrease in J_0 under the same V from Eq. 12. Therefore, P_{max} and η_T increase with increasing E_g from 0 to 2 eV. P_{max} can be expressed as

$$P_{max} = FF \cdot J_{sc} \cdot V_{oc}, \quad (18)$$

where FF is the fill factor and can be calculated as [2]

$$FF = \frac{v_{oc} - \ln(v_{oc} + 0.72)}{v_{oc} + 1}, \quad (19)$$

where v_{oc} is the normalized open circuit voltage and equals to $V_{oc}/0.0258$. When E_g is >2 eV, the photovoltaic cell absorbs the photons with an energy of E ($E > E_g$). FF increases gradually with the increase in E_g by calculation. V_{oc} increases linearly [15]. Figure 3 shows that the luminescence spectrum of the ZnS:Cu phosphor layer is very narrow; consequently, J_{sc} does not decrease in the beginning and then decreases rapidly to zero with increase in E_g from 2 eV to infinity from Eq. 13. So P_{max} increases initially and then decreases with the increase in E_g. The preceding analysis indicates that with the increase in E_g, η_T initially increases and then decreases; E_g ranges from 2 and 2.64 eV to allow η_T to reach the maximum value. The MATLAB calculation indicates that when E_g is equal to 2.075 eV, η_T reaches the maximum value at different H.

The aforementioned results and analysis indicate that emphasis should be placed on the thickness of the phosphor layer and the match between the luminescence spectrum and E_g of the photovoltaic cell in the preparation of the beta radioluminescence nuclear battery. The battery can exhibit good output performance if the thickness of the phosphor layer is set appropriately and if the luminescence spectrum matches the E_g of the photovoltaic cell.

Output performance and conversion efficiency

From the above results, the optimal parameters of the nuclear battery and output performance when the two portions of the battery are connected in a series are shown in Table 1.

The conversion efficiency of the beta radioluminescence nuclear battery may be expressed as

$$\eta_T = \eta_\beta \cdot \eta_{\beta-l} \cdot \eta_{l-el}, \quad (20)$$

Table 1 Optimal parameters and output performance of the battery

H_{op} (mg cm^{-2})	E_g (eV)	P_{max} (μW cm^{-2})	I_{sc} (μA cm^{-2})	V_{oc} (V)
11	2.075	44.24	15.1	3.19

Table 2 Battery conversion efficiency

η_T (%)	η_β (%)	$\eta_{\beta-l}$ (%)	η_{l-el} (%)
2.547	51	8.243	60.587

where $\eta_{\beta-l}$ is the conversion efficiency of the energy of the beta flux emitted from the surface of the ^{147}Pm source to the intensity of luminescence emitted from the external surface of the ZnS:Cu phosphor layer, and η_{l-el} is the conversion efficiency of luminescence intensity to electrical energy. The conversion efficiency under the condition of optimal parameters is shown in Table 2.

As shown in Table 2, the highest loss in efficiency in the battery occurs in the transport process of luminescence. The radioluminescence efficiency of the ZnS:Cu phosphor is approximately equal to 19 % [12], which is $>\eta_{\beta-l}$. This low value of $\eta_{\beta-l}$ is due to the fact that luminescence is absorbed by the phosphor layer and the source. To fully utilize the luminescence, a reflector can be added to the middle of the source and the phosphor layer to reflect back the luminescence emitted from the internal surface of the phosphor layer toward the photovoltaic cell. η_β may increase by reducing D_L.

Experiment verification

ZnS:Cu phosphor layers were fabricated on quartz glasses using physical sediment method [18] (Fig. 6a). The triple junction GaAs photovoltaic cell was purchased from Shenzhen Yin Xuan Sheng Technology Co., Ltd. The

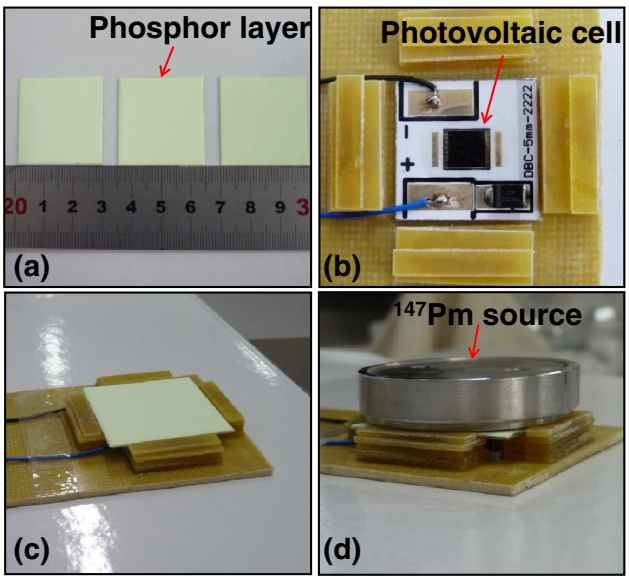

Fig. 6 Radioluminescence nuclear battery prototype setup

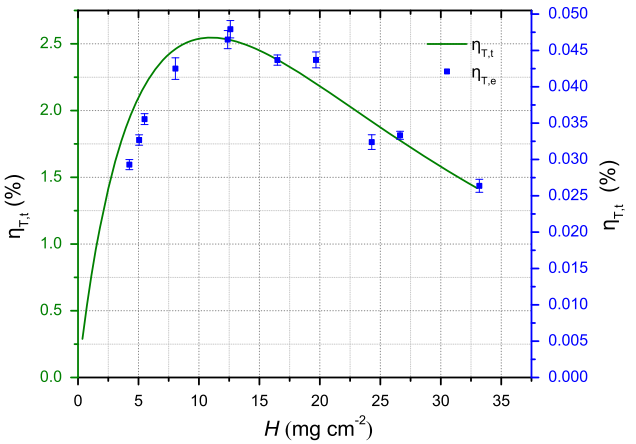

Fig. 7 Experimental and theoretical calculation values of total conversion efficiency

source is a single-track ^{147}Pm source with a density of activity of 5 mCi cm^{-2}. The radioluminescence nuclear battery prototype is shown in Fig. 6d. The current–voltages (I–V) were measured with a dual-channel system source meter instrument (Model 2636A, Keithley, USA). Given that E_g of photovoltaic cell does not affect the optimal thickness of the phosphor layer (Fig. 5), the experiment can be utilized to verify the accuracy of the theoretical calculation for the optimal thickness of the ZnS:Cu phosphor layer. Figure 7 shows the comparison of the experimental ($\eta_{T,e}$) and theoretical calculation values ($\eta_{T,t}$) of total conversion efficiency.

In the comparison with experiment, the numbers do not match up well but the trends do (Fig. 7). $\eta_{T,t}$ initially increases and then decreases with the increase in H. The optimal thickness of the phosphor layer was established. Similar trends were observed in the experiment; however, the optimal thickness exhibits a slight deviation. The possible reason for this deviation can be explained as follows. In the theoretical calculation, we described the ^{147}Pm source with a purity of 100 % and utilized the beta energy spectrum of ^{147}Pm directly. The ^{147}Pm source (in the form of Pm_2O_3) utilized in the experiment was prepared through powder metallurgy method [19]. The active block of ^{147}Pm contains abundant gold or silver powder and is sealed in a stainless steel shell. Owing to the gold powder, silver powder, and metal film that absorbs the low-energy electron, the beta energy spectrum hardens and the penetration distance of the beta particles becomes longer than that of the theoretical calculation. Therefore, the experimental results show a shift in the positive direction compared with the theoretical calculation in terms of the optimal thickness of the phosphor layer.

The maximum conversion efficiency of the battery in the experiment is only 0.048 %. Several factors affect the gap of conversion efficiency between the experimental results and the theoretical values. These factors include the different self-absorption, activity, and type (single-track or bidirectional) of the ^{147}Pm source and several simplifications in the theoretical calculation.

Conclusion

The optimal parameters, output performance, and conversion efficiency of a beta radioluminescence nuclear battery based on a sandwich-structure ^{147}Pm/ZnS:Cu/photovoltaic cell were determined by theoretical calculation. Under the parameters of D_L of 5.92 mg cm^{-2}, H_{op} of 11 mg cm^{-2}, and optimal E_g of 2.075 eV, the battery produces I_{sc} of 15.1 μA cm^{-2}, V_{oc} of 3.19 V and P_{max} of 44.24 μW cm^{-2} at 2.547 % η_T. Battery prototypes were fabricated and tested to verify the accuracy of the theoretical calculation for the optimal thickness of the phosphor layer. The theoretical and experimental values fit well. However, the conversion efficiency in the experiment is significantly lower than that in the theoretical calculation. Enhancing the activity of the source and adding a reflector between the source and the phosphor layer can improve the conversion efficiency.

Acknowledgments Supported by the National Natural Science Foundation of China (Grant No. 11205088), the Aeronautical Science Foundation of China (Grant No. 2012ZB52021), the Fundamental Research Funds for the Central Universities, and the Foundation of Graduate Innovation Center in NUAA (Grant No. kfjj130125).

References

1. Liu YP, Tang XB, Xu ZH, Hong L, Wang P, Chen D (2014) Optimization and temperature effects on sandwich betavoltaic microbattery. Sci China Technol Sci 57(1):14–18. doi:10.1007/s11431-013-5413-0
2. Tang XB, Liu YP, Ding D, Chen D (2012) Optimization design of GaN betavoltaic microbattery. Sci China Technol Sci 55(3):659–664. doi:10.1007/s11431-011-4739-8
3. Cress CD, Redino CS, Landi BJ, Raffaelle RP (2008) Alpha-particle-induced luminescence of rare-earth-doped Y_2O_3 nanophosphors. J Solid State Chem 181(8):2041–2045. doi:10.1016/j.jssc.2008.04.024
4. Walko RJ, Ashley CS, Brinker CJ, Reed ST (1990) Electronic and photonic power applications. The radioluminescent lighting technology transfer conference
5. Sims PE, Dinetta LC, Barnett AM (1994) High efficiency GaP power conversion for Betavoltaic applications. In: 13th Space photovoltaic research and technology conference, vol 1, pp 373-382
6. Sychov M, Kavetsky A, Yakubova G, Walter G, Yousaf S, Lin Q, Chan D, Socarras H (2008) Alpha indirect conversion radioisotope power source. Appl Radiat Isot 66(2):173–177. doi:10.1016/j.apradiso.2007.09.004
7. Prelas MA, Charlson EJ, Charlson EM, Meese J, Popovici G, Stacy T (1993) Diamond photovoltaic energy conversion. Second

international conference on the application of diamond films and related materials
8. Prelas MA, Popovici G, Khasawinah S, Sung J (1995) In: Prelas MA, Gielisse P, Popovici G, Spitsyn BV, Stacy T (ed) Wide band-gap photovoltaics, Kluwer Academic Publishers, Dordrecht
9. Schott RJ (2013) Photon intermediate direct energy conversion using a ^{90}Sr beta source. Nucl Technol 181(2):349–353
10. Weaver CL (2012) PIDECα: photon intermediate direct energy conversion using the alpha emitter polonium-210. University of Missouri–Columbia
11. Prelas MA, Boody FP, Miley GH, Kunze JF (1988) Nuclear driven flashlamps. Laser Part Beams 6(1):25–62. doi:10.1017/S0263034600003803
12. Bower KE, Barbanel YA, Shreter YG, Bohnert GW (2002) Polymers, phosphors, and voltaics for radioisotope microbatteries. CRC Press, Boca Raton, London, New York, Washington D.C
13. Smith WJ (1966) Modern optical engineering. McGraw-Hill, New York
14. Aronson JR, Emslie AG (1973) Spectral reflectance and emittance of particulate materials. 2: application and results. Appl Opt 12(11):2573–2584. doi:10.1364/AO.12.002573
15. Nelson J (2003) The physics of solar cells. Imperial College, London
16. Guo H, Lal A (2003) Nanopower betavoltaic microbatteries. In: Proceedings of 12th International conference on transducers, solid-state sensors, actuators and microsystems. doi:10.1109/SENSOR.2003.1215247
17. Katz L, Penfold AS (1952) Range-energy relations for electrons and the determination of beta-ray end-point energies by absorption. Rev Mod Phys 24(1):28. doi:10.1103/RevModPhys.24.28
18. Qin HF, Guo TL (2008) Preparation of tetrapod-shaped ZnO nanomaterial field emission cathodes by deposition method. Acta Phys Sin 57(2):1224–1228. doi:10.7498/aps.57.1224
19. Raybould D, Morris DG, Cooper GA (1979) A new powder metallurgy method. J Mater Sci 14(10):2523–2526. doi:10.1007/BF00737047